# XXIV. NOISE IN ELECTRON DEVICES*

Prof. R. B. Adler
Prof. H. A. Haus
Prof. J. B. Wiesner
R. P. Rafuse

## RESEARCH OBJECTIVES

While our work on the general problem of noise in linear networks came to a conclusion with the publication of Technology Press Research Monograph No. 2, "Circuit Theory of Linear Noisy Networks," by H. A. Haus and R. B. Adler (published jointly by the Technology Press of Massachusetts Institute of Technology and John Wiley and Sons, Inc., New York, 1959), related special problems continue to emerge. These are conveniently handled by the general methods developed in the monograph, and we shall continue to present applications of the general theory to cases of current interest as they arise.

R. B. Adler

## A. MEASUREMENT OF ABSOLUTE NOISE PERFORMANCE OF PARAMETRIC AMPLIFIERS

Any measurement procedure that is used to determine the absolute noise performance of a negative-resistance amplifier must necessarily include the behavior of the amplifier in cascade. For practical considerations (bandwidth, nonlinearity, and so on), one of the members of the cascade usually is chosen to be a unilateral, and inherently noisy, amplifier of a class whose normal performance is not as good as the capabilities of the parametric amplifier. This situation is, in fact, encountered if a negative-resistance amplifier is added to an existing system in order to improve its noise performance.

It should be noted that devices with negative-real input and/or output impedances, as well as positive-real devices driven from sources with negative-real impedances, are capable of being characterized and analyzed within the framework of exchangeable gain, noise figure, and noise measure (1). A suitable model for a generalized unilateral noisy amplifier (2, 3) is shown in Fig. XXIV-1. The excess exchangeable noise figure for this representation is

$$(F-1) = (R_n/R_g) + G_nR_g + 2\rho(R_nG_n)^{1/2} \tag{1}$$

where

*This research was supported in part by Purchase Order DDL-B222 with Lincoln Laboratory, a center for research operated by M.I.T., which is supported by the U.S. Air Force under Air Force Contract AF19(604)-5200.

$$\rho = \frac{\overline{e_n i_n}}{\left(\overline{e_n^2}\,\overline{i_n^2}\right)^{1/2}}$$

Figure XXIV-2 illustrates the behavior of (F-1) versus source resistance. The two minimum magnitude excess noise figures are

$$(F_+ - 1) = 2(1+\rho)(R_n G_n)^{1/2} \tag{2}$$

$$(F_- - 1) = -2(1-\rho)(R_n G_n)^{1/2} \tag{3}$$

for $R_{g,\,opt} = \pm(R_n/G_n)^{1/2}$, respectively. Penfield has derived a simple model for the signal-frequency behavior of a lossy varactor (4, 5). He also has shown that the best performance is obtained with the diode series resistance as the total idler circuit load. Figure XXIV-3 gives two models for the signal-frequency behavior of a lossy varactor for which

$m$ = Penfield modulation ratio ($m_{max} < 1/\pi$)

$\omega_c$ = diode cutoff frequency = $1/R_s C_{min}$

$\omega_i$ = idler frequency

$\omega_s$ = signal frequency

$R_s$ = series loss

$C_o$ = average capacity

$$R_d = -\frac{m^2 \omega_c^2}{\omega_i \omega_s} R_s \tag{4}$$

$$G_o = \frac{\dfrac{m^2 \omega_c^2}{\omega_i \omega_s} R_s \omega_s^2 C_o^2}{1 + \omega_s^2 C_o^2 \left(R_s - \dfrac{m^2 \omega_c^2}{\omega_i \omega_s} R_s\right)^2} \tag{5}$$

$$M_e = \frac{(F-1)}{1 - (1/G_e)} = \frac{\omega_s}{\omega_i}\frac{T_i}{T_o} - \frac{\omega_p}{\omega_i}\frac{T_i}{T_o}\frac{R_s}{R_s + R_d} \tag{6}$$

The best value of $M_e$ is obtained when $R_d = R_{d,\,max}$ (strong pumping).

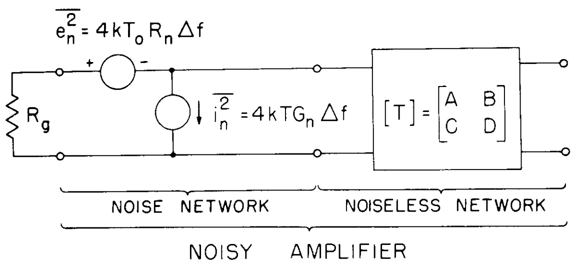


Fig. XXIV-1. Characterization of a noisy amplifier. Any linear noisy two-port can be separated into a noiseless two-port preceded by a pair of correlated noise generators.

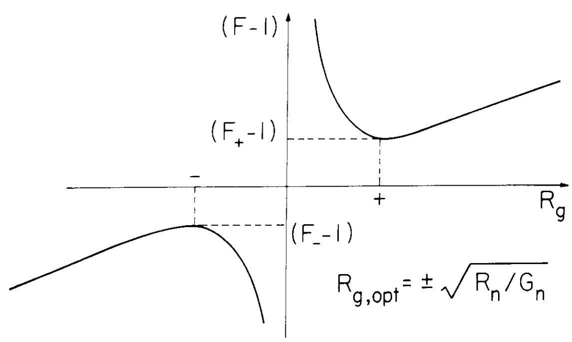


Fig. XXIV-2. Exchangeable excess noise figure. The two branches corresponding to $\pm R_g$ are particularly convenient when cascading. When the output impedance of the preceding stage is negative, its exchangeable gain is also negative, and a definite contribution to over-all noise-figure results.

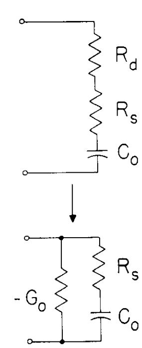


Fig. XXIV-3. Signal-frequency varactor models. A parallel equivalent circuit for the Penfield model is derived.

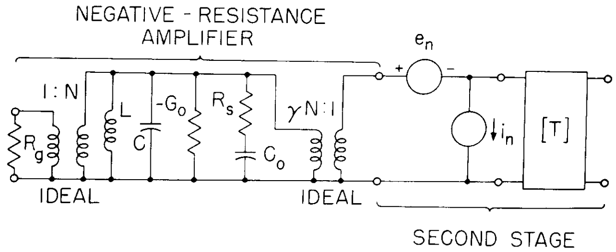


Fig. XXIV-4. Model of a negative-resistance amplifier in cascade with a noisy second stage. A signal-frequency model of a parametric amplifier is cascaded with a generalized noisy second stage. Two separate over-all noise figure expressions are necessary for the two regions.

Figure XXIV-4 presents a typical signal-frequency equivalent circuit for a "two-tank" parametric amplifier. The behavior of the cascade noise figure versus $R_g$ is characterized by two regions for $R_g \gtrless \left(N^2 G_{o,\,max}\right)^{-1}$. For $R_g > 1/N^2 G_{o,\,max}$

$$(F_{12}-1)_{G_{o,\,opt}} = \theta R_g + (\Gamma/R_g) + \Delta \tag{7}$$

and for $R_g < 1/N^2 G_{o,\,max}$

$$(F_{12}-1)_{G_{o,\,max}} = \Omega R_g + (\Phi/R_g) + X \tag{8}$$

where

$$(F_{12}-1) = (F_1-1) + \frac{(F_2-1)}{G_{e,\,1}}$$

It is apparent from the expression for noise measure of any cascade (1),

$$M_{e_{12}} = M_{e_1} + \Delta M_e \left( \frac{G_{e_2} - 1}{G_{e_{12}} - 1} \right) \tag{9}$$

that if $M_{e,\,1}$ is optimized by making $R_d = R_{d,\,max}$, then $M_{e,\,12}$ is optimized by making $\Delta M_e$ a minimum and $G_{e,1}$ a maximum. This may be achieved in practice by pumping the varactor as hard as possible (achieving $m_{max}$), adjusting the turns ratio of the first transformer, N, in such a way that $N^2 R_g \approx (G_{o,\,max})^{-1}$ $(G_{e,\,1} \to \infty)$, and simultaneously adjusting the second transformer turns ratio $\gamma N \to \infty$, with the result that the impedance seen by the second stage is $R_{g,\,opt}$ (from Fig. XXIV-2). The over-all exchangeable gain will be infinite in the limit, and $M_{e,\,12}$ reduces to $(F_{12}-1)$.

The calculated values of $\theta$, $\Gamma$, $\Delta$, $\Phi$, $\Omega$, and X necessary to predict the cascade noise figure for non-optimum conditions are:

$$\theta = \left\{(1-\rho^2)\frac{G_n}{\gamma^2} + \frac{\omega_p}{\omega_i}\frac{T_i}{T_o}\left[N^2\left(aR_s - a^2R_s^3\right) - \frac{R_sG_n}{\gamma^4N^2R_n} + \frac{\omega_s}{\omega_i}\frac{T_i}{T_o}\frac{a(R_s)^2}{2\gamma^2R_n}\right]\right.$$

$$+\left(\frac{\omega_p}{\omega_i}\frac{T_i}{T_o}\right)^2\left(\frac{aR_s^2 - 2a^2R_s^4}{\gamma^2R_n}\right) - \frac{1}{4\gamma^2R_n}\left(\frac{\omega_s}{\omega_i}\frac{T_i}{T_o}\right)^2$$

$$\left.+\frac{\rho}{\gamma^2}(G_n/R_n)^{1/2}\left(\frac{1}{2}+\frac{\omega_s}{\omega_i}\frac{T_i}{T_o}\right)\right\} \bigg/ 1 + \frac{\omega_p}{\omega_i}\frac{T_i}{T_o}\frac{R_s}{[\gamma N]^2R_n} \tag{10}$$

$$\Gamma = \frac{\frac{\omega_p}{\omega_i}\frac{T_i}{T_o}\frac{1}{N^2}R_s}{1 + \frac{\omega_p}{\omega_i}\frac{T_i}{T_o}\frac{R_s}{[\gamma N]^2R_n}} \tag{11}$$

$$\Delta = \frac{\frac{\omega_s}{\omega_i}\frac{T_i}{T_o} + \frac{\omega_p}{\omega_i}\frac{T_i}{T_o}\left[aR_s^2 + \frac{2\rho R_s}{(\gamma N)^2}(G_n/R_n)^{1/2}\right]}{1 + \frac{\omega_p}{\omega_i}\frac{T_i}{T_o}\frac{R_s}{(\gamma N)^2R_n}} \tag{12}$$

where

$$a = \frac{\omega_s^2C_o^2}{1+\omega_s^2C_o^2R_s^2}$$

These values are calculated under the constraint that $G_o$ is always adjusted (by varying the pump amplitude) so that the over-all noise figure is a minimum for any $R_g$ (provided that $G_{o,\,max}$ is not reached). The other parameters

$$\Phi = \gamma^2R_n \tag{13}$$

$$\Omega = \frac{\omega_s}{\omega_i}\frac{T_i}{T_o}N^2G_{o_{max}} + \frac{\omega_p}{\omega_i}\frac{T_i}{T_o}\left(N^2R_sG_{o_{max}} + aR_sN^2 - aR_s^2N^2G_{o_{max}}\right)$$

$$+ \gamma^2N^4R_nG_{o_{max}}^2 + G_n - 2\rho(R_nG_n)^{1/2}N^2G_{o_{max}} \tag{14}$$

$$X = 2\rho(R_nG_n)^{1/2} - 2(\gamma N)^2R_nG_{o_{max}} \tag{15}$$

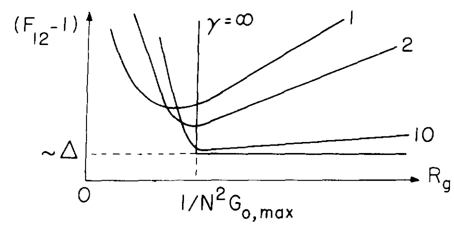


Fig. XXIV-5. Theoretical behavior of cascade noise figure versus $R_g$ and $\gamma$.

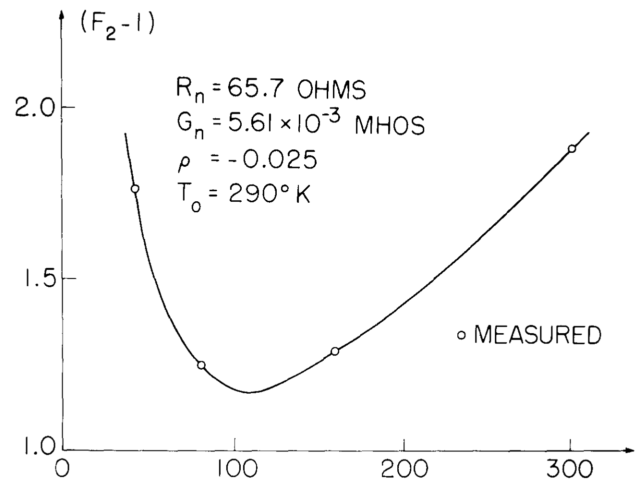


Fig. XXIV-6. Excess noise figure for an experimental second stage; $(F_2-1)$ versus source resistance was measured for a typical 108-mc receiver. The values of $R_n$, $G_n$, and $\rho$ are calculated from the measured values, and the curve is drawn from these values.

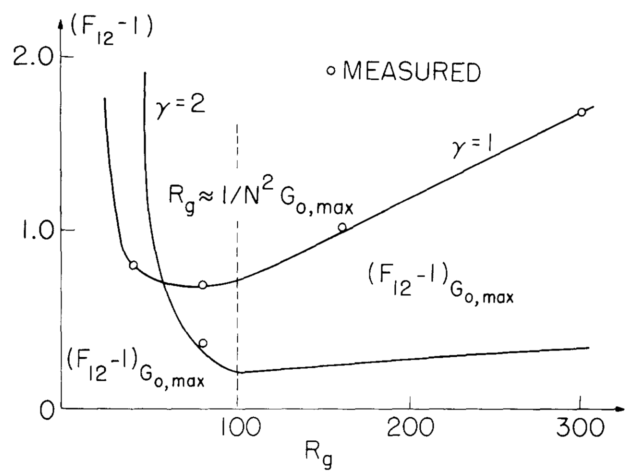


Fig. XXIV-7. Theoretical and experimental behavior of over-all excess noise figure. The theoretical noise-figure performance for an experimental cascade is compared with the measured performance.

hold for values of $R_g < \left(N^2 G_{o,\max}\right)^{-1}$.

Illustrated in Fig. XXIV-5 is the behavior of $(F_{12}-1)$ versus $\gamma$ and $R_g$. For practical reasons, it is necessary to know the extent to which the optimization procedure should be continued for a given varactor and a given second stage. These relations (Eqs. 10-15) are all that are necessary.

Table XXIV-1. Numerical values of $\Delta$, $\theta$, $\Gamma$, X, $\Omega$, and $\Phi$. From the necessary elements characterizing an experimental negative-resistance amplifier, and those derived from the second stage, a set of numerical values for the six basic parameters are derived. These are shown for two values of $\gamma$.

| $\gamma = 1$ | | $\gamma = 2$ | |
|---|---|---|---|
| $\Phi = 65.7$ | $\Gamma = 4.5 \times 10^{-2}$ | $\Phi = 252.8$ | $\Gamma = 4.5 \times 10^{-2}$ |
| $\Omega = 1.4 \times 10^{-2}$ | $\theta = 5.3 \times 10^{-3}$ | $\Omega = 3.0 \times 10^{-2}$ | $\theta = 1.32 \times 10^{-3}$ |
| $X = -1.28$ | $\Delta = 0.14$ | $X = -5.33$ | $\Delta = 0.14$ |

Figures XXIV-6 and XXIV-7 and Table XXIV-1 contain data on a specific experimental cascade. It is apparent that $(F_{12}-1)_{\text{best}}$ is nearly achieved by a combination of $R_g = 100$ ohms (with $N^2 = 50$) and $\gamma = 2$. It is interesting to note that, if the signal circuit is loaded too heavily (N small), a much poorer performance results. The agreement between theory and experiment indicates that the models chosen are adequate; the optimization procedure is evident from the curves of Fig. XXIV-7.

In conclusion, it can be shown that, as $\gamma$ becomes very large, $\Gamma$, $\theta$, and $\Delta$ reduce to

$$\Gamma \approx \frac{\omega_p T_i R_s}{\omega_i T_o N^2} \tag{16}$$

$$\theta \approx N^2 \frac{\omega_p T_i}{\omega_i T_o} \left(aR_s - a^2 R_s^3\right) \tag{17}$$

$$\Delta \approx \frac{\omega_s}{\omega_i} \frac{T_i}{T_o} + \frac{\omega_p}{\omega_i} \frac{T_i}{T_o}\, aR_s^2 \tag{18}$$

These values result in

$$(F_{12}-1)_{\text{opt}} \approx \frac{\omega_s}{\omega_i} \frac{T_i}{T_o} + \frac{\omega_p}{\omega_i} \frac{T_i}{T_o} \left(aR_s^2 - a^2 R_s^4\right)^{1/2} \text{ for } R_{g,\text{opt}} \approx \left[N^2\left(a - a^2 R_s^2\right)\right]^{-1/2} \tag{19}$$

R. P. Rafuse

References

1. H. A. Haus and R. B. Adler, Circuit Theory of Linear Noisy Networks (The Technology Press, Cambridge, Mass., and John Wiley and Sons, Inc., New York, 1950).

2. A. G. Th. Becking, H. Groendijk, and K. S. Knol, The noise factor of 4-terminal networks, Philips Research Reports 10, 349-357 (1955).

3. H. Rothe and W. Dahlke, Theory of noisy four-poles, Proc. IRE 44, 811-817 (1956).

4. H. A. Haus and P. Penfield, Jr., On the noise performance of parametric amplifiers, Internal Memorandum No. 19, Energy Conversion Group, Department of Electrical Engineering, M.I.T., Aug. 11, 1959 (unpublished).

5. P. Penfield, Jr., Interpretation of some varactor amplifier noise formulas, Internal Memorandum, Microwave Associates, Inc., Burlington, Massachusetts, Sept. 1, 1959 (unpublished).